A&A 367, 321–325 (2001)
DOI: 10.1051/0004-6361:20000412

Astronomy & Astrophysics

On the MHD stability of the $m = 1$ kink mode in solar coronal loops

H. Baty

Observatoire Astronomique, 11 rue de l'Université, 67000 Strasbourg, France

Received 4 September 2000 / Accepted 15 November 2000

Abstract. We revisit the ideal MHD stability of the $m = 1$ kink mode in configurations representative of coronal loops, using a stability code. We adopt different magnetic force-free equilibria defined by the twist function that are embedded into an outer potential field situated at a radial distance r_0 from the magnetic axis. In the limit $r_0 \gg l_0$, l_0 being the axis pitch length, the configurations are driven unstable by the kink mode when the twist exceeds the classical critical value of 2.5π on the axis. However, the critical axis twist strongly depends on the equilibrium in the opposite limit, with sharply increasing values when r_0 becomes of the order or smaller than l_0. We interpret these results in terms of the stability criterion $\langle\Phi\rangle_l = 2.5\pi$, where $\langle\Phi\rangle_l$ is the twist value averaged over a radial length l. It is found that l is of the order of 3−4 times l_0, provided $r_0/l_0 \gtrsim 5$; otherwise it depends on the twist profile via the existence of magnetic resonances.

Key words. Sun: corona – MHD – methods: numerical – instabilities

1. Introduction

High resolution observations have shown that the solar corona displays many plasma loop-like structures of different sizes. It is believed that these coronal loops play a crucial role in the dynamics of solar flares and for heating the solar corona.

A coronal loop is a curved magnetic flux tube anchored in the photosphere. Because of the large density and small resistivity of the photospheric fluid, the magnetic field lines can be considered as frozen in the photospheric flow which twists the flux tube (injecting magnetic energy and electric current in the loop). However, this magnetic energy storage cannot proceed further when the loop becomes unstable on a fast time scale shorter than that of photospheric motions.

The MHD stability of different equilibrium models of coronal loops has been studied by a large number of authors (see Hood 1992 for a review). A stability analysis in ideal MHD has been recently performed by Van der Linden & Hood (1998, 1999) showing that the $m = 1$ (m being the azimuthal mode number) kink instability is always the first mode to become unstable for force-free equilibria. Note that, in the limit of a magnetically dominated solar corona, coronal loops are most probably best described via force-free fields. It is well established that loops are kink unstable when the amount of twist a threshold (Raadu 1972; Hood & Priest 1979; Einaudi & Van Hoven 1983; Velli et al. 1990). Thus, the critical twist value is 2.5π for the uniform-twist force-free field introduced by Gold & Hoyle (1960), while it depends on the details of the equilibrium for a more general configuration.

In this paper, we propose to revisit the ideal MHD $m = 1$ stability of force-free equilibria representative of twisted coronal loop configurations. Several papers have already investigated the kink stability of a variety of different equilibria. Indeed, Hood & Priest (1979) have considered equilibrium configurations defined by analytical expressions of the magnetic field components including plasma pressure, extending the results obtained for the uniform-twist force-free field to more realistic configurations. Einaudi & Van Hoven (1983) and Velli et al. (1990) have studied a family of current confined fields initially introduced by Chiuderi & Einaudi (1981). Here, we focus on four different equilibria defined by the radial variation of the twist function. In particular, we investigate the effect of the closeness and nature of an outer potential region. This study is mainly motivated by recent results showing the fundamental role played by the details of the twist profile and the outer potential field on the non linear development of kink instability (Baty et al. 1998; Lionello et al. 1998a). As in all the previously mentioned studies, we restrict our attention to the cylindrical geometry approximation. The computations are performed using the MHD stability code of Velli et al. (1990).

This paper is organized as follows. The equilibrium configurations and the numerical procedure are described

Send offprint requests to: H. Baty,
e-mail: baty@astro.u-strasbg.fr

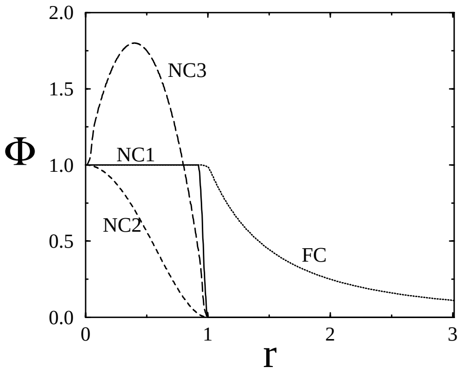

Fig. 1. The profiles of the magnetic twist Φ as a function of the radial distance to the magnetic axis r for the four equilibria considered. The twist is normalized to the value on the axis and the distance is expressed in units of r_0

in Sect. 2. In Sect. 3, we present and discuss the results. Finally, the conclusions are drawn in Sect. 4.

2. The equilibrium and numerical procedure

We consider axisymmetric force-free equilibria with a vanishing plasma pressure defined by the magnetic twist function Φ. For a flux tube of length L, the twist is given by the following expression:

$$\Phi(r) = \frac{LB_\theta}{rB_z}, \tag{1}$$

where B_θ and B_z are the azimuthal and axial components of the equilibrium magnetic field respectively. The radial variations of the equilibria adopted in the present study are plotted in Fig. 1. Note that, for all the configurations, the internal twisted region is embedded into an external potential field situated at a radial distance r_0. The three equilibria having a vanishing twist in the potential region (i.e. NC1, NC2, and NC3) carry a zero net electric current as a consequence of Ampère's law. This is not the case for the remaining equilibrium (FC), where the potential field decreases as $1/r$. As concerns the radial variation of the twist in the internal region, two configurations (NC1 and FC) have a constant twist value followed by transitions to zero and to a $1/r^2$ dependence respectively. For the NC2 case, we have adopted the following expression:

$$\Phi(r) = \Phi_0 \left(1 - \frac{r^2}{r_0^2}\right)^2, \tag{2}$$

valid for $0 \leq r \leq r_0$, that is similar to a case investigated by Mikic et al. (1990). Φ_0 is the twist on the axis. Finally, the equilibrium NC3 displays a non-monotonic variation given by:

$$\Phi(r) = \Phi_0 \left(1 + 4\frac{r}{r_0} - 5\frac{r^2}{r_0^2}\right), \tag{3}$$

valid for $0 \lesssim r \lesssim r_0$. Moreover, in order to avoid singularities of the density current in the transition region near r_0, the internal twist value (for cases NC1, NC3, and FC) is continuously matched to the potential field on a radial length scale much smaller than r_0 using a numerical spline procedure. The same procedure is used to have a zero derivative on the axis for the NC3 equilibrium. One must note that we restrict our attention to configurations having no reversal of B_z (see Velli et al. 1990 for equilibria with a B_z reversal). An artificial perfectly-conducting wall is placed at a radial distance $a > r_0$ in order to simplify the computations. Optimal (i.e. sufficiently high) values for a/r_0 have been chosen in order to give negligible effects on the results.

We have investigated the linear properties of these loops using a numerical stability code developed by Velli et al. (1990). This numerical approach is based on Fourier series expansion for the displacement (Einaudi & Van Hoven 1981):

$$\boldsymbol{\xi}(\boldsymbol{r}, t) = \boldsymbol{\xi}(\boldsymbol{r}) \exp(\gamma t), \tag{4}$$

$$\boldsymbol{\xi}(\boldsymbol{r}) = \Re \sum_n \boldsymbol{\xi_n}(r) \exp[i(m\theta + n\pi(z/L + 1))], \tag{5}$$

with γ representing the linear growth rate of the $m = 1$ kink mode. This technique is not particularly suited for line-tied geometry, and gives only an approximate solution (De Bruyne et al. 1990; Van der Linden et al. 1990; Hood et al. 1994). However, the code has been tested in a variety of topologically different magnetic configurations (Einaudi & Van Hoven 1983; Velli et al. 1990; Lionello et al. 1998b; Baty et al. 1998) that are kink unstable. It has been shown that five axial Fourier harmonics (given by n values) centered around a well chosen axial wavenumber are sufficient for an acceptable convergence (with a deviation of the order of a few percent) of the sum in Eq. (4). With the different parameters characterizing the equilibrium given, $\Phi(r)/L$ and r_0, it is possible to compute the linear growth rate γ as a function of the loop length L (see for example Fig. 3 in Baty et al. 1998). The threshold for the onset of the kink instability expressed in terms of the critical length (or equivalently in terms of the critical twist) can therefore be determined as the minimum value necessary to have $\gamma \gtrsim 0$.

3. Results

We have computed the critical twist value measured on the axis, Φ_c, as a function of the normalized distance $d = r_0/l_0$, where l_0 is the axis pitch length defined as the inverse of the twist per unit (loop) length on the axis Φ_0/L. The results are plotted in Fig. 2, and have been obtained using the optimal values $a/r_0 = 4$ for the null current equilibria (NC1, NC2, and NC3) and $a/r_0 = 8$ for the finite current one (FC).

For all the configurations, a constant asymptotic value close to 2.5π is determined in the limit $d \gg 1$. This means that, in this limit, the stability properties are essentially independent of the details of the magnetic configuration. Moreover, the solution is the classical one obtained for the uniform-twist force-free field (Gold & Hoyle 1960)

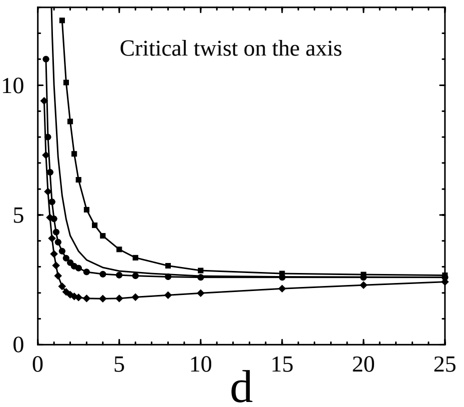

Fig. 2. The critical twist value on the axis in units of π as a function of the normalized distance $d = r_0/l_0$; for the NC1 (plain line), NC2 (squares), NC3 (diamonds), and FC (circles) equilibria

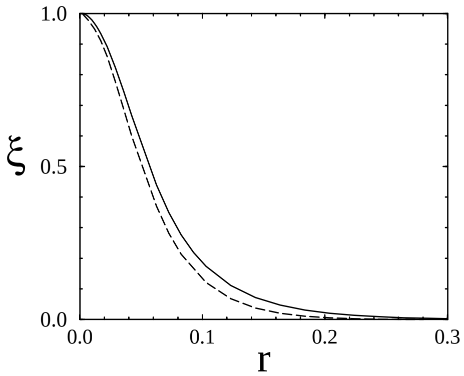

Fig. 3. The radial component of the linear displacement as a function of the radial distance r (normalized to r_0) for the NC1 (plain line) and for the NC3 (long-dashed) cases. A value $d = 20$ is chosen

(GH) and is given by the threshold value $\Phi_c = 2.5\pi$. This is not the case in the opposite limit, where the critical twist crucially depends on the equilibrium with drastically increasing values as d decreases.

Note that l_0 is also the characteristc length scale defining the radial variation of the magnetic field in the case of the GH equilibrium. Hence, the axial field component is given by:

$$B_z = \frac{B_0}{1 + r^2/l_0^2}, \quad (6)$$

B_0 being the magnitude of the magnetic field on the axis. Consequently, the results for the configurations having a constant twist in the internal region (NC1 and FC) can be easily interpreted. Indeed, when the potential field is situated far enough from the region containing the major part of the current that drives the instability (i.e. $r_0 \gg l_0$), negligible effects due to the potential field are expected compared with the solution of the GH equilibrium. However, when $r_0 \sim l_0$, the closeness of the potential region has a stabilizing effect and leads to an increasing critical twist value as d decreases. For a given value of d, the stabilization is more important for the NC1 case, because the twist is vanishing in the potential region leading to an average twist smaller than for the FC configuration. For the same Φ_0 value, a twist value $\langle\Phi\rangle_l$ averaged over a radial length l (that remains to be determined) is maximum for the GH case, lower for the FC case, and minimum for the NC1 equilibrium. Thus, introducing a stability condition $\langle\Phi\rangle_l = 2.5\pi$, Φ_c values higher than 2.5π are necessary to drive the configurations (FC and NC1) kink unstable.

Let us now turn to the results of the NC2 equilibrium. A constant asymptotic critical twist value close to 2.5π is obtained, but the convergence is achieved for higher values of d (i.e for $d \simeq 20$) than for the previously discussed cases. This can be explained by the fact that the twist function is not constant in the internal part of the flux tube and decreases monotically towards zero at r_0. For the same Φ_0 value, the average twist $\langle\Phi\rangle_l$ is smaller than for the previous configurations, requiring then a higher axis critical twist Φ_c for a given d. A similar configuration has been studied by Mikic et al. (1990) with $L/r_0 = 4$, where a critical axis twist value of the order of 4.8π has been obtained. This corresponds to a ratio $r_0/l_0 \simeq 3.77$, giving a critical twist of 4.65π (from Fig. 2) that is in rough agreement with Mikic et al.'s results. This result is interpreted in the literature (Robertson et al. 1992; Hood 1992) as the axis twist necessary to have $\langle\Phi\rangle_{r_0} \simeq 2.5\pi$. However, if one chooses a different d value, Fig. 2 shows that this stability criterion using r_0 as the averaging length does not work anymore. This also means that an expression $l \simeq 3.8 l_0$ is required in order to assess the stability criterion $\langle\Phi\rangle_l = 2.5\pi$ for the onset of the kink instability in this case.

For the last equilibrium (NC3), the 2.5π value is again obtained but the convergence is now achieved for $r_0/l_0 \simeq 30$. One must also note that the critical twist is lower than 2.5π over a large range of d values (typically for $d \gtrsim 1.3$) and that a minimum twist of order 1.65π is determined for $d \simeq 5$. This result can be mainly explained by the non-monotonic twist variation given by Eq. (3). Indeed, as a consequence, the average twist $\langle\Phi\rangle_l$ has a non monotonic variation as a function of l. Taking the following expression for the average twist:

$$\langle\Phi\rangle_l = \frac{\int_0^l \Phi(r)\,\mathrm{d}r}{l}, \quad (7)$$

one can easily find that $\langle\Phi\rangle_l$ is maximum for $l/r_0 = 0.6$ with a value equal to $1.6\Phi_0$. Therefore, according to the stability criterion $\langle\Phi\rangle_l = 2.5\pi$, a minimum axis critical twist of the order of 1.56π is expected, that is in rough agreement with our measured value. Moreover, this corresponds to a l value about $3l_0$, that is slightly lower compared to the previous estimate.

In order to obtain more information on the l expression, we have investigated the radial dependence of the linear displacement associated with kink instability. In Fig. 3, we have plotted the radial component of the displacement ξ at the loop apex for the NC1 and NC3 equilibria, using a rather high value for the normalized distance d

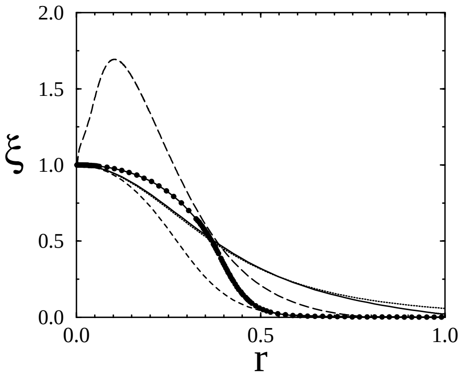

Fig. 4. The radial component of the linear displacement as a function of the radial distance for the four equilibria (using $d = 3$): NC1 (plain line), NC2 (dashed), NC3 (long-dashed), and FC (dotted). The radial component of the linear displacement is also plotted for the NC2 case using $d = 2$ (plain line with circles)

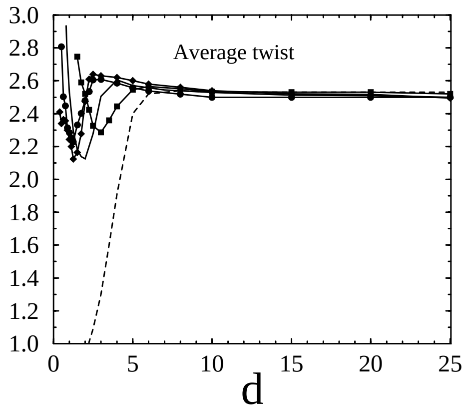

Fig. 5. The average twist $\langle \Phi \rangle_l$ (in units of π) as a function of d for the NC1 (plain line), NC2 (squares and dashed line), NC3 (diamonds) and FC (circles) equilibria. We use the critical twist values on the axis reported in Fig. 2, and adopt the expression given by Eq. (7) except for NC2 (dashed line) where Eq. (8) is used. We also use the optimal expression $l = 3.5 l_0$

(i.e. $d = 20$). One can see that the two curves are very similar, having a maximum on the axis and values falling off rapidly with r on a characteristic length scale of order $3{-}4\ l_0$ (i.e. $0.15 - 0.2\ r_0$). Note also that the results for the two other cases are not shown because they are undistinguishable from the NC1 one. We have checked that a similar conclusion can be drawn for other d values provided $d \gg 1$. However, a different situation is obtained when d is smaller. Indeed, one can easily see in Fig. 4 that the radial variation of ξ depends on the configuration for $d = 3$. While the displacement is well confined within the current channel region (i.e. within r_0) for the null current cases (NC1, NC2, and NC3), it invades the potential region for the finite current configuration (FC). A similar comment has been made by Lionello et al. (1998a) leading the authors to introduce a difference between an internal kink (for a null current equilibrium) and an global kink (for a finite current case) mode. Moreover, the instability is even more localized for the NC2 and NC3 equilibria with ξ being confined within a radius of order $0.4 r_0$ and $0.7 r_0$ respectively. It is also found that this limiting radius remains roughly the same when d becomes smaller, as is illustrated in Fig. 4 for the NC2 case with $d = 2$. These results obtained for small d values can be understood in terms of magnetic resonances, which are defined as regions where the radial component of the perturbed magnetic field vanishes. Indeed, it has been shown that, when a resonant point exists at a radius $r_{\rm s}$ located at the loop apex, the instability is mainly confined within $r_{\rm s}$ (Velli et al. 1990; Baty & Heyvaerts 1996; Baty et al. 1998). We have therefore checked that, while $r_{\rm s}$ is close to $0.4 r_0$ and to $0.7 r_0$ for the NC2 and NC3 cases respectively, it is of order r_0 for the two other equilibria. Moreover, this resonant point remains within the current channel for the null current configurations while it is situated in the potential region for the FC case. As a consequence, the averaging length l is probably affected when d becomes sufficiently small.

Finally, attempts to find a general expression for l have been unsuccessful. However, taking into account the previous estimates, one can say that l is probably of order $3{-}4\ l_0$ over a relatively large range of d values, regardless of the equilibrium. Assuming a given l expression, it is possible to compute the average twist $\langle \Phi \rangle_l$ defined by Eq. (7) using the critical axis twist values obtained in Fig. 2. As one can see in Fig. 5, we have therefore obtained that an optimal value $l = 3.5\ l_0$ provides the stability condition $\langle \Phi \rangle_l \approx 2.5\pi$ over a rather large range of d values (typically for $d \gtrsim 5$). Note that a different l expression leads to the same conclusion, provided $l \approx 3$–$4\ l_0$. When $d \lesssim 5$, the stability criterion is not fulfilled meaning that the l expression assumed is not valid. Moreover, Fig. 5 shows that the average twist is minimum (with values of the order of 2π) for $r_0/l_0 \approx 1$–3. This can be explained by the existence of resonances which prevent the l value from further increasing as r_0/l_0 decreases. The averaging length should be probably limited by $r_{\rm s}$ when d becomes of order 1, as suggested by the radial structure of the eigenfunctions. As the expression (given by Eq. (7)) used to calculate the average twist is somewhat arbitrary, we have also taken the following expression suggested by Velli et al. (1990):

$$\langle \Phi \rangle_l = \frac{\int_0^l L B_\theta \, {\rm d}r}{\int_0^l r B_z \, {\rm d}r}, \quad (8)$$

where r_0 has been replaced by l. The results using Eq. (8) are plotted in Fig. 5 for the NC2 case, using $l = 3.5\ l_0$. One can easily conclude that similar conclusions can be drawn, except that the deviation between our calculated twist values and 2.5π is stronger when d becomes of order 1.

4. Summary and conclusions

In this paper, we have investigated the ideal MHD stability of the kink mode in cylindrical equilibria representative of twisted coronal loops. We have adopted four different force-free magnetic configurations, that are defined by the twist function in the internal part, and that are confined by an external potential field situated at a radial distance r_0 from the axis.

Provided that the potential field is far enough from the central part of the internal twisted region, i.e. $r_0 \gg l_0$, the $m = 1$ kink mode drives the configurations unstable when the twist exceeds the classical critical value of 2.5π on the axis. This means that the stability properties, in this limit, are essentially independent of the details of the configuration. The solution is therefore the same as the one obtained for the uniform-twist force-free equilibrium. This is not the case when r_0 becomes of the order of or smaller than l_0, as the critical axis twist sharply increases as r_0/l_0 decreases.

Interpretations of the stability properties of the kink mode have been previously given in terms of the stability condition $\langle\Phi\rangle_{r_0} = 2.5\pi$, where $\langle\Phi\rangle_{r_0}$ is the twist averaged over the current channel region. We have shown that a similar criterion with r_0 replaced by another characteristic length l must be taken in order to understand our results. Indeed, adopting the expression $l \approx 3$–$4 \;\; l_0$, the stability criterion $\langle\Phi\rangle_l = 2.5\pi$ is retrieved for $r_0/l_0 \gtrsim 5$. However, this is no longer true when r_0/l_0 is smaller, because of the existence of magnetic resonances that confine the mode inside a resonant radius of order r_s. The r_s value depends on the configuration and is close to r_0 for loops having a uniform-like twist in the central region followed by a sharp transition to the potential field.

We believe that these results are important not only because they contribute to a better understanding of the stability properties of coronal loops, but they can serve as a useful guideline to predict where the current concentrations can form during the non-linear evolution of kink instability. Indeed, on the basis of non linear simulations (Baty et al. 1998), we suggest that the localization of the current layer should be probably given by a radial distance of order $l \simeq 3$–$4 \; l_0$ independently of the configuration for $r_0/l_0 \gtrsim 5$. This is not the case when $r_0/l_0 \lesssim 5$, because the existence of magnetic resonances (which depend on the twist profile) determine where the current concentration can form. This is an important point to understand the ensuing reconnection process and the associated change of magnetic toplology (Baty 2000a, 2000b).

Acknowledgements. The author thanks Marco Velli for having giving him the possibility to use the stability code, and Jean Heyvaerts for fruitful discussions. We also thank the anonymous referee for fruitful criticisms that helped improve the content of the paper.

References

Baty, H., & Heyvaerts, J. 1996, A&A, 308, 935
Baty, H., Einaudi, G., Lionello, G., & Velli, M. 1998, A&A, 333, 313
Baty, H. 2000a, A&A, 353, 1074
Baty, H. 2000b, A&A, 360, 345
Chiuderi, C., & Einaudi, G. 1981, Solar Phys., 73, 89
De Bruyne, P., Velli, M., & Hood, A. W. 1990, Comp. Phys. Comm., 59, 55
Einaudi, G., & Van Hoven, G. 1981, Phys. Fluids, 24, 1092
Einaudi, G., & Van Hoven, G. 1983, Solar Phys., 88, 163
Gold, T., & Hoyle, F. 1960, MNRAS, 120, 89
Hood, A. W., & Priest, E. R. 1979, Solar Phys., 64, 303
Hood, A. W. 1992, Plasma Phys. & Contr. Fusion, 34, 411
Hood, A. W., De Bruyne, P., Van der Linden, R. A. M., & Goossens, M. 1994, Solar Phys., 150, 99
Lionello, R., Velli, M., Einaudi, G., & Mikic, Z. 1998a, ApJ, 494, 840
Lionello, R., Schnack, D. D., Einaudi, G., & Velli, M. 1998b, Phys. Plasmas, 10, 3722
Mikic, Z., Schnack, D. D., & Van Hoven, G. 1990, ApJ, 361, 690
Raadu, M. 1972, Solar Phys., 22, 425
Robertson, J. A., Hood, A. W., & Lothian, R. M. 1992, Solar Phys., 137, 273
Van der Linden, R. A. M., Goossens, M., & Kerner, W. 1990, Comp. Phys. Comm., 59, 61
Van der Linden, R. A. M., & Hood, A. W. 1998, A&A, 339, 887
Van der Linden, R. A. M., & Hood, A. W. 1999, A&A, 346, 303
Velli, M., Einaudi, G., & Hood, A. W. 1990, ApJ, 350, 428